NASA TECHNICAL MEMORANDUM NASA TM 75190

INSTABILITY OF A COMPRESSIBLE CIRCULAR FREE JET WITH CONSIDERATION OF THE INFLUENCE OF THE JET BOUNDARY LAYER THICKNESS

Alfons Michalke

Translation of "Instabilität eines kompressiblen runden Frestrahls unter Berücksichtigung des Einflusses der Strahlgrenzschichtdicke", Zeitschrift für Flugwissenschaften, Vol. 19, No. 8/9, 1971, pp. 319 - 328.

NATIONAL AERONAUTICS AND SPACE ADMINISTRATION
WASHINGTON, D.C. DECEMBER 1977

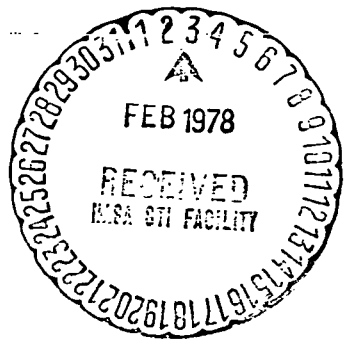

STANDARD TITLE PAGE

1. Report No.	2. Government Accession No.	3. Recipient's Catalog No.
NASA TM 75190		

4. Title and Subtitle	5. Report Date
Instability of a compressible circular free jet with consideration of the influence of the jet boundary layer	December 1977
	6. Performing Organization Code

7. Author(s)	8. Performing Organization Report No.
Alfons Michalke	
	10. Work Unit No.

9. Performing Organization Name and Address	11. Contract or Grant No.
SCITRAN Box 5456 Santa Barbara, CA 93108	NASw-2791
	13. Type of Report and Period Covered
12. Sponsoring Agency Name and Address National Aeronautics and Space Administration Washington, D.C. 20546	Translation
	14. Sponsoring Agency Code

15. Supplementary Notes: Translation of "Instabilität eines kompressiblen runden Frestrahls unter Berücksichtigung des Einflusses der Strahlgrenzschichtdicke." Zeitschrift für Flugwissenschaften, Vol. 19, No. 8/9, 1971, pp. 319 - 328.

16. Abstract: The instability of a circular jet is investigated by means of the inviscid linearized stability theory. By variation of a jet parameter which takes the ratio of jet radius to boundary layer thickness into account, the influence of axisymmetry on the spatial growth rate and disturbance phase velocity is studied. Furthermore, the influence of Mach number and temperature ratio is discussed. A comparison with measurements shows that the instability of a turbulent jet boundary layer may also be explained by these results.

17. Key Words (Selected by Author(s))	18. Distribution Statement
	Unclassified - Unlimited

19. Security Classif. (of this report)	20. Security Classif. (of this page)	21. No. of Pages	22. Price
Unclassified	Unclassified	25	

INSTABILITY OF A COMPRESSIBLE CIRCULAR FREE JET WITH CONSIDERATION OF THE INFLUENCE OF THE JET BOUNDARY LAYER THICKNESS

Alfons Michalke†

/31

SUMMARY

The instability of a circular jet is investigated by means of the inviscid linearized stability theory. By variation of a jet parameter which takes the ratio of jet radius to boundary layer thickness into account, the influence of axisymmetry on the spatial growth rate and disturbance phase velocity is studied. Furthermore, the influence of the Mach number and temperature ratio is discussed. A comparison with measurements shows that the instability of a turbulent jet boundary layer may also be explained by these results.

1. INTRODUCTION

The instability of a circular free jet with respect to small perturbations caused by acoustic waves was observed by J. Tyndall [1]. Lord Rayleigh [2] made a theoretical analysis of this instability using an idealized round free jet which is produced by a circular vortex layer. The result of this theoretical investigation where the friction was ignored confirms the instability of the round free jet with respect to axisymmetric perturbations.

During the 1930's, G. B. Brown [3] concerned himself with the instability of a plane-free jet and the related vortex creation. The laminar-turbulent transition in a circular free jet was considered again in 1952 by R. Wille [4]. A large number of experimental and theoretical papers of the free jet instability were performed (see [5-30]) under his direction at the Hermann Foettinger Institute for Fluid Mechanics of the Technical University, Berlin, and later at the D. F.

*Numbers in margin indicate pagination in foreign text.

V. L. R. Institute for Turbulence Research in Berlin. A. J. Reynolds [31], H. A. Becker, and T. A. Massaro [32] concerned themselves with the phenomena associated with vortex formation in a circular free jet. The organ pipe tones of a circular free jet was investigated by A. B. C. Anderson [34, 35].

In general, a circular free jet consists of a potential jet core where the jet velocity is constant as well as a jet boundary layer which surrounds the jet core and within which the velocity decreases from its maximum value to zero. For Reynolds numbers on the order of $Re = 10^4$, the flow near the nozzle mouth is approximately parallel. The Reynolds number is referred to the maximum jet velocity and nozzle diameter. In addition, in the vicinity of the nozzle, the thickness of the free jet boundary layer is very small compared with the free jet diameter.

For the theoretical treatment of the free jet instability, usually the following assumptions were made:

I. The influence of friction is negligible for the stability calculations. This means that the frictionless linearized perturbation equations can be used.

II. The undisturbed free jet can be considered as a parallel flow which is infinite upstream and downstream, and only has an axial velocity component.

III. The boundary layer of the free jet and the inflection point of the velocity profile determines the instability. This means that for a small boundary layer thickness compared with the free jet diameter, one can ignore the axial symmetry of the free jet. This means that the free jet boundary layer can be replaced by a plane free shear layer.

Assumption I was confirmed by experiments of H. Schade and A. Michalke [13], as well as P. Freymuth [21, 23] for a round-free jet, and by H. Sato [36] as well as A. Michalke and R. Wille [22] for the plane free jet. Theoretical results for the free jet instability were also derived by A Michalke [16, 20] using the assumptions I to III. P. Freymuth [21, 23] compared the results with experiments and it was found that there was agreement only when the so-called space excitation perturbation was assumed in the theory, such as in [20]. Here we are dealing with wave perturbations, whose amplitudes increased exponentially in the direction of the free jet. Already M. Gaster [37, 38] pointed out that instead of using the conventional time excitation perturbations of classical

stability theory, only space excitation perturbations would make physical sense for free boundary layers.

The agreement between the theory and the experiment was quite good /320 for small frequency perturbations. At higher frequencies there were deviations, which were explained by A. Michalke [28] using the condition that assumption II was violated. In a free-jet emerging from a nozzle, the flow is not exactly parallel because the velocity distribution changes from the wall boundary layer profile in the nozzle into the free jet profile with the inflection point. This profile conversion in the flow direction apparently is not important for perturbations with a small frequency and a large wavelength. Apparently it does influence the instability mechanism considerably for perturbations with a high frequency and a small wavelength.

The limitations of the theoretical treatment of the free jet instability by ignoring the axial symmetry (assumption III) are for the most part unknown. The approximate investigations of this influence by A. Michalke and H. Schade indicated that especially for small frequencies and/or relatively thick free jet boundary layers, the axial symmetry cannot be ignored. This is obvious because then the perturbation wavelength is on the order of the free jet diameter.

The theoretical investigation of this influence of axial symmetry on the instability of a round free jet is the topic of this paper. Using the assumptions I and II, we will discuss the free jet instability and we will drop the assumption III. The calculation is based on space excitation perturbations which make physical sense. The compressibility of the medium is considered in order to investigate the influence of the Mach number and a temperature distribution on the free jet instability. This influence was already investigated by H. Gropengeiser [26] and W. Blumen [39] for a plane free shear layer.

Lord Rayleigh [2] and H. Schade [10] considered the instability of a round free jet, as well as G. K. Batchelor and A. E. Gill [40]. A. E. Gill [40] as well as A. Michalke and H. Schade [13] calculated the eigenvalues for the incompressible free jets with a simple velocity profile. M. Lessen, J. A. Fox and H. M. Zein [41], as well as A. E. Gill [42] investigated the influence of the Mach number on the instability of the cylindrical vortex layer. T. Kambe [43] considered the influence of the Reynolds number on the instability of a circular free jet with parabolic velocity profile. All of these investigations

assumed perturbations which are excited in time. For perturbations excited in space, the instability of the cylindrical vortex layer was discussed by A. Michalke [30] as well as S. C. Crow and F. H. Champagne [44]. The results for these "ideal" round free jets with zero boundary layer thickness showed considerable deviations with earlier results calculated for perturbations excited in time. Therefore it seems appropriate to expand the stability investigation to circular free jets with finite boundary layer thickness.

The meaning of the instability of the laminar boundary layer for the creation of turbulence in a circular free jet is certainly well known. Apparently, not only is the laminar free jet boundary layer unstable, but a turbulent free jet boundary layer is also unstable. Experiments by S. C. Crow and F. H. Champagne [44] showed, that a turbulent free jet boundary layer also undergoes an instability process. Just like in the laminar case, there are wave components excited in space which lead to the formation of turbulent ring vortices. This instability of the turbulent-free jet boundary layer which can be observed in a region up to about six nozzle diameters behind the nozzle could be very important for the sound production mechanism in the free jet. This is because the region of the free jet producing the sound is influenced substantially by this instability. The experimental wavelengths of the perturbations found are greater than the free jet diameter and the frequencies are very small. Therefore, for the theoretical investigation of this instability, it can be assumed that the high frequency turbulent fluctuation motion in the turbulent boundary layer can be ignored as a first approximation, and that only the average velocity profile is important. This velocity profile in the important region (about two nozzle diameters downstream of the nozzle) has a relatively thick boundary layer. Therefore, in a stability calculation, the axial symmetry certainly cannot be ignored. In this sense, the results of the present paper are also applicable to the instability of the turbulent-free jet boundary layer if the parameters are appropriately selected.

In section 2 we will first discuss the undisturbed flow in a circular free jet, whose instability will be investigated. In section 3, we will discuss the solution of the instability problem, and in section 4 we will discuss the results.

2. THE UNDISTURBED FLOW IN A CIRCULAR FREE JET

In order to describe the flow field in a circular free jet, we will use a cylindrical coordinate system x, r, φ, where the x-axis points in the free jet axis direction. The velocity components are then c_x, c_r, c_φ. The velocity distribution in the undisturbed free jet can be assumed to be parallel according to assumption II for large Reynolds numbers. Within this approximation, the free jet only has an axial velocity component U(r) which is independent of x. At the jet axis r = 0, we have $U(o) = U_1$, whereas outside $U(r) \to 0$ for $r \to \infty$. The free jet radius R is called the radius for which the velocity is reduced to one-half of the maximum value, that is, $U(R) = U_1/2$.

The undisturbed free jet can also have a temperature profile T(r), where the absolute temperature below the jet axis is $T(o) = T_1$ and in the surroundings we have $T(\infty) = T_0$. If the speed of sound along the jet axis corresponding to T_1 is called a_1, and if T_0 corresponds to a_o, then the local speed of sound a(r) is given by:

$$a(r) = a_1 \sqrt{T(r)/T_1}. \tag{2.1}$$

The pressure p_o is constant in the undisturbed free jet. Therefore we obtain the density distribution as follows from the state equation for ideal gases: /321

$$\varrho(r) = \varrho_1 T_1/T(r). \tag{2.2}$$

ρ_1 is the density along the free jet axis. ρ_o is the density of the surrounding medium at rest, and we obtain the following for the temperature ratio T*:

$$T^* = T_0/T_1 = \varrho_1/\varrho_0 = (a_0/a_1)^2. \tag{2.3}$$

The Mach number of the free jet is defined by

$$M = U_1/a_1. \tag{2.4}$$

In general, the velocity and temperature profiles are not independent in the boundary layer. Just like in the paper by H. Gropengeisser [26], the temperature-velocity coupling is assumed according to Busemann-Crocco Law:

$$T(r) = T_1\left[T^* + (1 - T^*)\frac{U(r)}{U_1} + \frac{\gamma - 1}{2} M^2 \frac{U(r)}{U_1}\left(1 - \frac{U(r)}{U_1}\right)\right]. \tag{2.5}$$

Here γ is the ratio of these specific heats. Relationship (2.5) applies

for a Prandtl number Pr = 1 and a constant specific heat.

The momentum loss boundary layer thickness ϑ is used as the characteristic of the free jet boundary layer. For the compressible free jet boundary layer, it is defined as follows:

$$\vartheta = \int_0^\infty \frac{\bar{\varrho}(r)}{\varrho_1} \frac{U(r)}{U_1}\left(1 - \frac{U(r)}{U_1}\right) dr. \tag{2.6}$$

Because of (2.2) and (2.5), ϑ depends on the velocity profile U(r) and the Mach number M and the temperature ratio T*.

We can give a physically meaningful function for the velocity profile U(r). Here we will not investigate free jets with well-developed velocity profiles, but free jet profiles with a relatively large potential jet core, as can be found just behind the nozzle mouth. In addition, the profiles must have an analytical description. In the following, we will carry out the calculation of the free jet instability for two simple analytic velocity profiles.

The velocity profile 1 is defined by the following:

$$\frac{U(r)}{U_1} = \begin{cases} 1 & \text{for } 0 \leqq r < R - \frac{\delta}{2}, \\ \frac{1}{2}\left\{1 + \tanh\left[b_1\left(1 - \frac{r}{R}\right)\right]\right\} & \\ & \text{for } R - \frac{\delta}{2} < r \leqq \infty, \end{cases} \tag{2.7}$$

where the value $\delta < 2R$ must be so large that the discontinuity in the profile at $r = R - \delta/2$ can be ignored, that is, $\tanh b_1 \delta/2\ R) \sim 1$. The quantity b_1 is a measure for the velocity gradient or for the boundary layer thickness.

The velocity profile 2 is defined by:

$$\frac{U(r)}{U_1} = \frac{1}{2}\left\{1 + \tanh\left[b_2\left(\frac{R}{r} - \frac{r}{R}\right)\right]\right\}, \tag{2.8}$$

which is valid over the entire range $0 \leq r \leq \infty$. The quantity b_2 is also a measure for the boundary layer thickness.

The velocity profiles and also the temperature profiles, according to (2.5), depend on r/R and a free jet parameter R/ϑ which is a measure for the ratio of the jet radius and the jet boundary layer thickness. R/ϑ is considered a characteristic variable for the influence of the axial symmetry on the instability of the free jet in the following. For a specified free jet parameter value R/ϑ it is possible to calculate b_1 and b_2 using (2.6). We then obtain the following for profile

1:

$$b_1 = \frac{R}{\vartheta} f(M, T^*), \tag{2.9}$$

where $y = U(r)/U_1$ is the boundary layer function f defined by

$$\begin{cases} f(M, T^*) = \frac{1}{2}\int_0^1 \left[T^* + (1 - T^*)\, y + \right. \\ \qquad \left. + \frac{\gamma - 1}{2} M^2 y (1 - y) \right]^{-1} dy \end{cases} \tag{2.10}$$

This integral can be solved in closed form.

For profile 2, we obtain an explicit solution for b_2 only for the temperature ratio $T^* = 1$. In this case, we have

$$b_2 = \frac{1}{2} \frac{R}{\vartheta} f(M, T^* = 1). \tag{2.11}$$

The variation of the boundary layer function f as a function of the Mach number M is shown in Figure 1 for the temperature ratios $T^* = 1$ and $T^* = 0.5$. We have assumed a value for air ($\gamma = 1.4$) for the ratio of the specific heats, which will also be maintained in the following stability calculations.

The velocity profiles 1 and 2 can be calculated for fixed free jet parameters R/ϑ using (2.9) and (2.11). Figure 2 shows the velocity profiles for $M = 0$ and $T^* = 1$ for different values of R/ϑ. The velo-

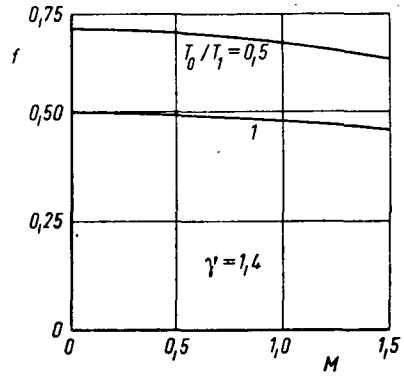

Figure 1: Boundary function f as a function of the Mach number M for $\gamma = 1.4$ and two values of the temperature ratio T_o/T_1.

city profiles 1 are anti-symmetric with respect to the value r = R, and the profiles 2 are asymmmetric. For $R/\vartheta = 12{,}5$, we can see the relatively small differences for both profile shapes. Velocity profiles with $R/\vartheta = 50$ to 100 are typical for the free jet region near the nozzle mouth where the laminar-transition occurs. On the other hand, profiles with $R/\vartheta < 12{,}5$ should be important for the instability of turbulent free jet boundary layers.

In Figure 3, we show the velocity and temperature profiles for a single Mach number M = 1.2 and one temperature ratio T* = 1 for $R/\vartheta = 100$ and 6.25. The velocity profiles are slightly flatter than for M = 0 (see Figure 2) because of the smaller value of f (see Figure 1). The

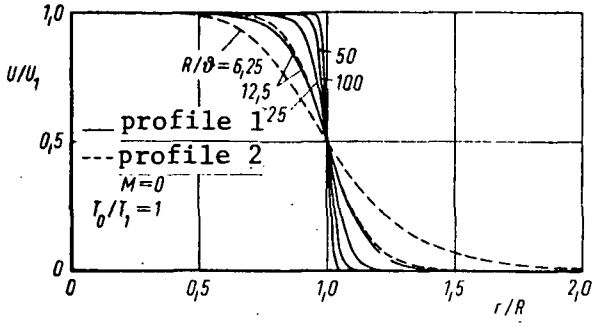

Figure 2: Velocity profiles 1 and 2 at the Mach number M = 0 and the temperature ratio T_0/T_1 for various values of the free jet parameter R/ϑ.

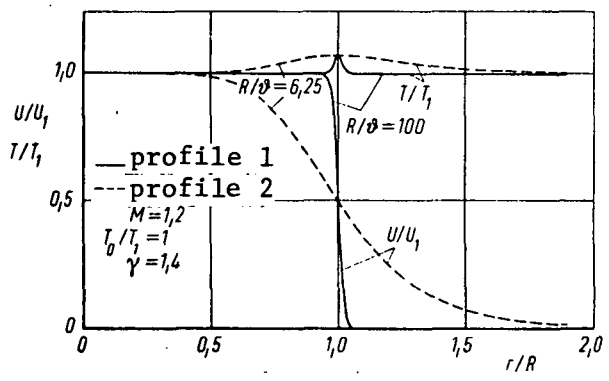

Figure 3: Velocity and temperature profiles in air (γ = 1.4) for two values of the free jet parameter R/ϑ for a Mach number M = 1.2 and temperature ratio T_0/T_1 = 1.

maximum of the temperature in the boundary layer thickness is a consequence of the aerodynamic heating at higher Mach numbers.

For a hot free jet, the velocity and temperature profiles are shown in Figure 4. Here, we have M = 0 and T* = 0.5. The velocity profile 1 for $R/\vartheta = 50$ and 25 is steeper than for T* = 1 (see Figure 2) because of the larger value of f (see Figure 1).

For a fixed ϑ the free jet profile 1 becomes the plane hyperbolic tangent velocity profile for $R \to \infty$ which was investigated for stability by A. Michalke. In the following, we will perform stability calculations for the velocity profiles shown in Figures 2 through 4.

3. SOLUTION OF THE INSTABILITY PROBLEM

3.1 The Perturbation Differential Equations

In order to investigate instability we will superimpose small perturbations $(c_x', c_r', c_\varphi', p', \varrho')$ on to the parallel flow of the undisturbed free jet. It is assumed that the Prandtl number Pr = 1. Since also the Reynolds number was assumed to be very large, we can use the frictionless equations of motion (assumption I). Also in this case the entropy of the flowing particles remains constant during the motion. The linearized flow equations were derived with these assumptions in [30]. Because of the linearity of the perturbation equations, it is then sufficient to consider the behavior of single-wave perturbations. One trial solution which is compatible with the equations is

$$\begin{cases} [c_x', c_r', c_\varphi', p', \varrho'] = \\ \quad = [\tilde{u}(r), \tilde{v}(r), \tilde{w}(r), \tilde{p}(r), \tilde{\varrho}(r)]\, e^{i(\alpha x + m\varphi - \beta t)}. \end{cases} \tag{3.1}$$

For perturbations excited in space, which are the only ones considered here, the circular frequency β and the whole azimuth wave number m of the perturbation are real, whereas $\alpha = \alpha_r + i\alpha_i$ is in general complex. α_r is the axial wave number of the perturbation and $-\alpha_i > 0$ is its buildup factor in space. For m = 0, we have axisymmetric perturbations, and for m = 1 we have the first azimuthal perturbation, etc.

Using the trial solution (3.1), we eliminate the amplitude functions $\tilde{u}(r)$, $\tilde{w}(r)$ and $\tilde{\varrho}(r)$ from the linearized perturbations. According to [30], we obtain the following differential equation system for the amplitude functions $\tilde{v}(r)$ and $\tilde{p}(r)$:

$$\begin{cases} i\alpha\bar{\varrho}\left[\left(U - \frac{\beta}{\alpha}\right)\frac{1}{r}\frac{d(r\tilde{v})}{dr} - \frac{dU}{dr}\tilde{v}\right] = \\ \qquad\qquad = -\left[\lambda^2 + \left(\frac{m}{r}\right)^2\right]\tilde{p}, \end{cases} \tag{3.2}$$

$$i\alpha\bar{\varrho}\left(U - \frac{\beta}{\alpha}\right)\tilde{v} = -\frac{d\tilde{p}}{dr}, \tag{3.3}$$

where we have used the abbreviation

$$\lambda^2 = \alpha^2\left[1 - \left(\frac{U - \beta/\alpha}{a}\right)^2\right] \tag{3.4}$$

As a boundary condition for the instability problem, we must require that perturbations, that is the solutions of (3.2) and (3.3), are regular at r = 0 and vanish for $r \to \infty$. Therefore, we have to solve the following eigenvalue problem: For a specified basic flow, U(r), $\bar{\varrho}(r)$

and a(r) and the prescribed values of m and β, we must determine the complex eigenvalue α in such a way that the boundary conditions are satisfied.

For $r \to 0$, we have $U \to U_1$, $\tilde{\rho} \to \rho_1$, and $a \to a_1$. The asymptotic solution for the pressure amplitude which satisfies the boundary condition at r = 0 is then the following for $r \to 0$:

$$\tilde{p}(r) \sim I_m(\lambda_1 r). \tag{3.5}$$

Here, I_m is the modified vessel function of the first kind of order m and λ_1 is the value of $\lambda(0)$ according to (3.4) with a positive real part.

For $r \to \infty$, we have $U \to 0$, $\tilde{\rho} \to \rho_0$ and $a \to a_0$. The asymptotic solution which satisfies the second boundary condition is the following for $r \to \infty$: /32

$$\tilde{p}(r) \sim K_m(\lambda_0 r), \tag{3.6}$$

where K_m is the modified vessel function of the second kind of order m and λ_0 is the value of $\lambda(\infty)$ with a positive real part.

3.2 Numerical Solution of the Eigenvalue Problem

The eigenvalue problem can only be solved numerically for the velocity profiles 1 and 2 of section 2. Therefore, the equation system (3.2) and (3.3) should be converted. By introducing the function

$$\chi(r) = -i\alpha\tilde{p}(r)/\tilde{v}(r), \tag{3.7}$$

which was also used by H. Gropengeisser [26] we obtain a complex nonlinear differential equation of first order,

$$\begin{cases} \dfrac{d\chi}{dr} = -\alpha^2\bar{\varrho}\left(U - \dfrac{\beta}{\alpha}\right) + \\ \quad + \chi\left\{\dfrac{1}{U-\beta/\alpha}\left[\dfrac{\lambda^2 + (m/r)^2}{\alpha^2\bar{\varrho}}\chi - \dfrac{dU}{dr}\right] + \dfrac{1}{r}\right\}. \end{cases} \tag{3.8}$$

For sufficiently small or large r, in the square bracket the quantity dU/dr can be ignored compared with the first term. The asymptotic behavior of the function X can be calculated from (3.5) or (3.6) and (3.3). If the corresponding radii are called r_1 and r_0, then we obtain

$$\chi(r_1) = -\frac{\alpha^2\varrho_1(U_1 - \beta/\alpha)}{\lambda_1}\frac{I_m(\lambda_1 r_1)}{I_m'(\lambda_1 r_1)} \tag{3.9}$$

as well as

(3.10) $$\chi(r_0) = \frac{\varrho_0 \alpha \beta}{\lambda_0} \frac{K_m(\lambda_0 r_0)}{K_m'(\lambda_0 r_0)},$$

where I_m' and K_m' are the derivatives of the functions I_m and K_m and with respect to their argument. For the velocity profile 1, we select $r_1 = R = \delta/2$ and $r_o = R + \delta/2$.

For an arbitrarily-selected value pair α differential equation (3.8) with the initial value (3.9) can be numerically integrated from $r = r_1$ to $r = R$. It can be indicated with the initial value (3.10) from $r = r_o$ to $r = R$. For the correct eigenvalue α, the difference of the two solutions will be 0 at $r = R$. This can be used to solve the eigenvalue problem using a zero-point method for complex functions.

The integration of the complex differential equation (3.8) was done using a Runge-Kutta method, which determines the local optimum step for a prescribed accuracy*. The zero method is based on complex parabolic interpolation. A subprogram for calculating the modified Bessel functions with complex arguments was used to calculate the initial values (3.9 and 3.10). It is known that [11] the boundary layer thickness is a characteristic length for the instability of a free boundary layer. Therefore, the momentum loss boundary layer thickness ϑ is selected as a reference length for the instability problem. The reference velocity selected is the free jet velocity U_1. The normalized complex eigenvalues $\alpha\vartheta$ depend on the azimuth wave number m, the normalized frequency or Strouhal number $\beta\vartheta/U_i$ and the flow parameters R/ϑ, M and T*. Calculations for the axisymmetric and first azimuth perturbations were first made for M = 0 and T* = 1 with the free jet parameter values R/ϑ = 100, 50, 25, 12.5 and 6.25 in order to investigate the influence of axial symmetry on the incompressible free jet. For T* = 1 and R/ϑ = 100, and 6.25, we calculated for M = 0.4, 0.8, and 1.2 in order to study the influence of the Mach number on the instability behavior. The instability of a hot free jet with T* = 0.5 and $R/\vartheta = 50$ and 25 were also calculated for the Mach number M = 0.

3.3 Instability Behavior of a Round Free Jet for Very Small Frequencies.

P. G. Drazin and L. N. Howard [45] showed that a plane free shear

*The numerical calcuations were done on a digital computer, Zuse Z-23, made available by the German Research Federation, Bonn-Bad, Godesberg.

layer behaves like a plane vortex layer with respect to two-dimensional perturbations at very low frequencies. The special form of the velocity profile of the shear layer then no longer is important. However, this is not true for three-dimensional perturbations [27, 26]. Therefore, we could expect that a circular free jet will behave like a cylindrical vortex layer with respect to axisymmetric perturbations at very small freuencies. The investigation of the instability of the cylindrical vortex layer excitation is space was done by A. Michalke [30] as well as S. C. Crow and F. H. Champagne [44]. The result is that in addition to the "regular" perturbation mode with $\alpha \to 0$ for $\beta \to 0$, there are other "irregular" perturbation modes which for $\beta \to 0$ give a buildup factor $\alpha_i > 0$ which is different from zero. The physical meaning of this "irregular perturbation mode", however, is not clarified. Since these modes have not yet been observed in experiments, it is natural to believe that these solutions are a consequence of an infinite parallel flow (assumption II).

For an incompressible circular free jet with a velocity profile 1 for $R/\vartheta = 50$, we compared the calculated eigenvalues $\alpha_r\vartheta$ and $-\alpha_i\vartheta$ of the axisymmetric perturbation m = 0, with the results for the cylindrical vortex layer for a small $\beta\vartheta/U_1$ value. The curves are given in Figure 5. For the "regular" mode I, it can be seen that the continuous velocity profile 1 does indeed behave like a cylindrical vortex layer for $\beta\vartheta/U_1 \to 0$ and large values of R/ϑ. Therefore, for small frequencies, the phase velocity $c_{ph} = \beta/\alpha_r$ of the axisymmetric perturbation is greater than the jet velocity U_1. The "irregular" perturbation modes also occur for the continuous velocity profile 1, and the first mode will be called II. For this mode II, the cylindrical vortex layer is a good approximation. Approximately for $\beta\vartheta/U_1 = 0{,}04$, the wave number α_r of mode II in Figure 5 becomes zero. Therefore its phase velocity $C_{ph} = \beta/\alpha$ becomes infinite. Physically speaking, this "irregular" mode II is probably meaningless, as already mentioned. /324

For three-dimensional perturbations with $m \geq 1$, even for $\beta = 0$, the special velocity profile of the free jet influences the eigenvalues. In order to calculate these eigenvalues for $\beta = 0$, we use the following function in the differential equation (3.8) and in the boundary conditions (3.9) and (3.10), and we introduce the new eigenvalue

(3.11) $$\bar{\chi} = \chi/\alpha^2$$

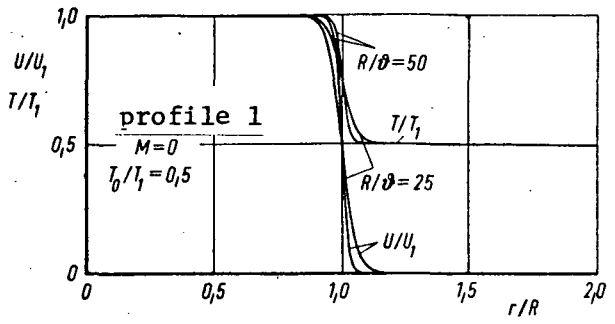

Figure 4: Velocity and temperature profiles for 2 values of the free jet parameter R/ϑ for a Mach number M = 0 and a temperature ratio of $T_o/T_1 = 0.5$.

(3.12). $$c = \beta/\alpha$$

It is assumed that c remains finite for $\beta \to 0$. In the limiting case $\beta = 0$ the eigenvalue c for $m \geq 1$ is calculated from the differential equation

(3.13)
$$\begin{cases} \dfrac{dX}{dr} = -\bar{\varrho}(U-c)\overline{+} \\ \qquad + X\left\{\dfrac{1}{U-c}\left[\dfrac{1}{\bar{\varrho}}\left(\dfrac{m}{r}\right)^2 X - \dfrac{dU}{dr}\right] + \dfrac{1}{r}\right\} \end{cases}$$

with the boundary value

(3.14)
$$\begin{cases} X(r_1) = -\varrho_1 (U_1 - c)\, r_1\, m^{-1}, \\ X(r_0) = -\varrho_0\, c\, r_0\, m^{-1}. \end{cases}$$

The influence of the Mach number on the instability expressed by the function λ^2 according to (3.4) no longer occurs in this limiting case.

For the first azimuth perturbation of the velocity profiles, the ratios $\alpha_r U_1/\beta$ and $-\alpha_i U_1/\beta$ are shown on Figure 6 as a function of $\beta\vartheta/U_1 \to 0$ for M = 0 and T* = 1. This is compared with the results for the cylindrical vortex layer. The free jet parameter here is $R/\vartheta = 100$ and 25. It can be seen that these values are different, even for $\beta = 0$ and the deviation is greater for smaller values of R/ϑ. It is found that just like for the plane shear layer [27], the phase velocity C_{ph} of the three-dimensional perturbation is smaller than the jet velocity U_1 for the limiting value $\beta = 0$.

4. DISCUSSION OF RESULTS

4.1 Influence of Free Jet Parameter on the Instability of an Incompressible Circular Free Jet.

We assume an incompressible free jet if the Mach number is M = 0, and the temperature ratio is T* = 1. For this case we will first investigate the influence of axial symmetry expressed by the free jet parameter R/ϑ . The instability problem for the velocity profile 1 and using the substitution

(4.1) $$r = R - \eta$$

in (2.7), as well as the differential equation (3.8) and the boundary values (3.9) and (3.10), for $R \to \infty$, can be reduced to the instability problem of the plane hyperbolic tangent shear layer profile, which was solved in [20]. The eigenvalue curves for this case, therefore, are the limiting curves for the instability of the free jet profile 1 for $R/\vartheta \to \infty$.

Figure 7 shows, as a function of the normalized frequency $\beta\vartheta/U_1$, the normalized phase velocity c_{ph}/U_1 and the normalized build-up factor $-\alpha_i\vartheta$ of the axisymmetric "regular" perturbation (m = 0) for different free jet parameter values R/ϑ . For $R/\vartheta = 100$, the buildup factor $-\alpha_i\vartheta$ differs only very slightly from the values for $R/\vartheta = \infty$, and the axial symmetry can be ignored here. The same is true for the phase velocity c_{ph}/U_1 for values $\beta\vartheta/U_1 > 0.1$. For smaller frequencies, the phase velocity deviates greatly from the values of the plane shear layer $(R/\vartheta = \infty)$ and becomes greater than the jet velocity, such as was the case for /325 the cylindrical vortex layer [30, 44]. Therefore, the influence of axial symmetry on the phase velocity for small frequencies cannot be ignored, even for a free jet with large R/ϑ .

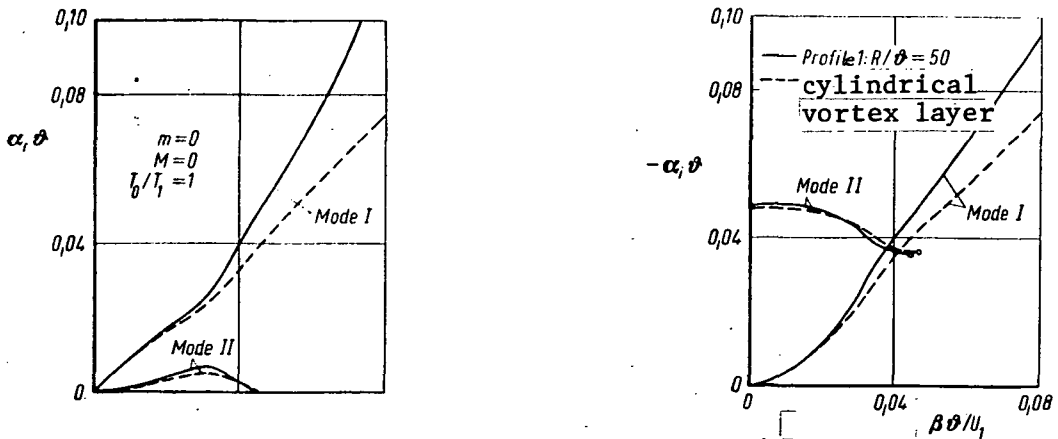

Figure 5: Comparison of eigenvalues α_r and $-\alpha_i$ of an axisymmetric perturbation for profile 1 with those of the cylindrical vortex layer at $R/\vartheta = 50$ for small circular frequencies β(M = 0, T_0/T_1 = 1)

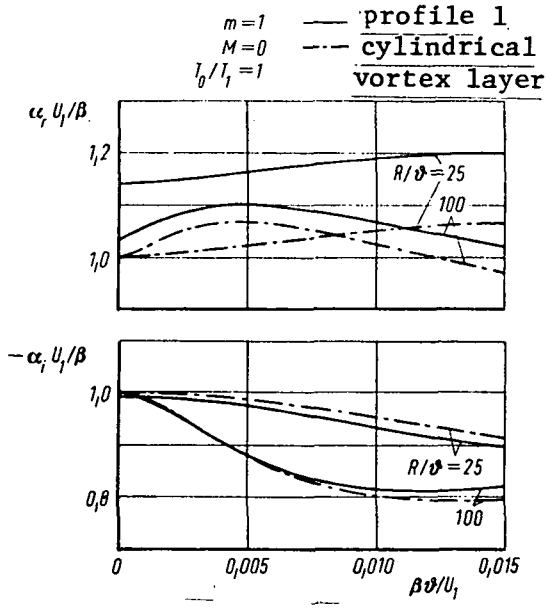

Figure 6: Comparison of eigenvalue α_r and $-\alpha_i$ of the first azimuthal perturbation for profile 1 with those of the cylindrical vortex layer $R/\vartheta = 100$ and 25 for small circular frequencies β($M = 0$, $T_o/T_1 = 1.$)

For smaller R/ϑ values, the maximum of the phase velocity decreases and at the same time the maximum of the buildup factor becomes smaller and is displaced towards larger $\beta\vartheta/U_1$ values. In other words, the increasing influence of axial symmetry reduces the instability of the free jet. In Figues 7 and for $R/\vartheta = 12{,}5$, we show the curves for the velocity profile 1 and for the profile 2. One can see, especially for the curves $-\alpha_i\vartheta$, that even for small R/ϑ the shape of the velocity profile has a subatantial influence on the free jet instability.

The frequencies in a round-free jet are often characterized by the Strouhal number S_D formed with the nozzle diameter D. If we set approximately D = 2R for the free jets considered here, then this Strouhal number S_D is related to $\beta\vartheta/U_1$ as follows:

$$S_D = \frac{1}{\pi}\,\frac{\beta\vartheta}{U_1}\,\frac{R}{\vartheta}. \tag{4.2}$$

Therefore, we obtain the order of the Strouhal number range of $S_D < 8$ and a maximum buildup occurs at $S_D = 3$ for $R/\vartheta = 100$. For $R/\vartheta = 6{,}25$, the instability region is given by $S_d < 0.65$ with a maximum buildup at about $S_D = 0.35$.

According to P. Freymuth [21, 23] the Strouhal number range for $R/\vartheta = 100$ is characteristic for laminar-turbulent transition. According

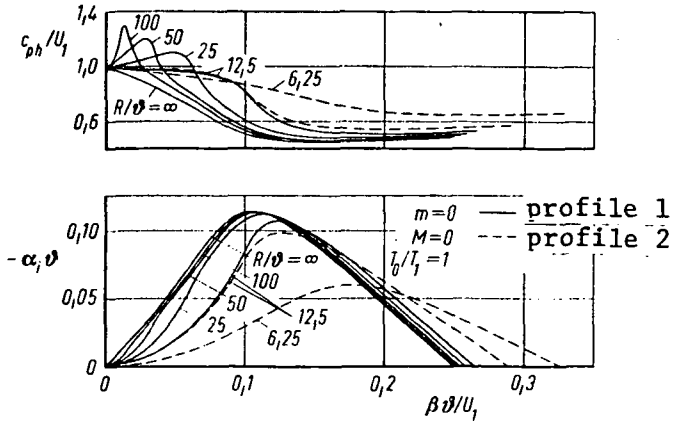

Figure 7: Phase velocity c_{ph} and buildup factor $-\alpha_i$ of the asymmetric perturbation as a function of circular frequency β for various free jet parameter values R/ϑ $(M=0,\ T_0/T_1=1)$

to S. C. Crow and F. H. Champagne [44], the range for $R/\vartheta=6{,}25$ is characteristic of the instability of the turbulent free jet boundary layer.

Figure 8 shows that this instability of the free turbulent boundary layer does indeed approximately follow the linearized theory. Here we show the phase velocity of the axisymmetric perturbations in the turbulent free jet measured in [44] as a function of the Strouhal number S_D. In addition, we show the theoretical curves for the velocity profile 2 with $R/\vartheta=12{,}5$ and 6.25. The last curve corresponds approximately to the average velocity profile which was measured by S. C. Crow and F. H. Champagne [44] at the distance x = 2D behind the nozzle. The relatively good agreement of measured values of phase velocity and the position of maximum buildup with the theoretical values for $R/\vartheta=6{,}25$ shows that in [44], it was erroneously believed that the theory of space buildup of perturbations had failed. S. C. Crow and F. H. Champagne [44] reached this conclusion by comparing their measured and theoretical values for cylindrical vortex layers. It was found that perturbations excited in time resulted in a better agreement with the measured values than perturbations excited in space. From Figure 8, it can be seen that it is not the theory of perturbations excited in space which fails, but that the approximation of replacing a free jet boundary layer profile with approximately $R/\vartheta=6$ by means of a cylindrical vortex layer is not permissible.

For the non-axisymmetric perturbations with $m \geq 1$, for $R \to \infty$, the influence of the axial symmetry vanishes as does the dependence on M.

For $R/\vartheta = \infty$, the two-dimensional perturbation of the plane free jet also results in limiting curves for m $\geq$ 1. Figure 9 shows the normalized phase velocity and the buildup factor for the same free jet parameter values R/ϑ as in Figure 7, as a function of $\beta\vartheta/U_1$. The phase velocity here in general is smaller than U_1, especially for $\beta\vartheta/U_1 \to 0$. As a comparison with Figure 7 shows, the curves of phase velocity for m = 0

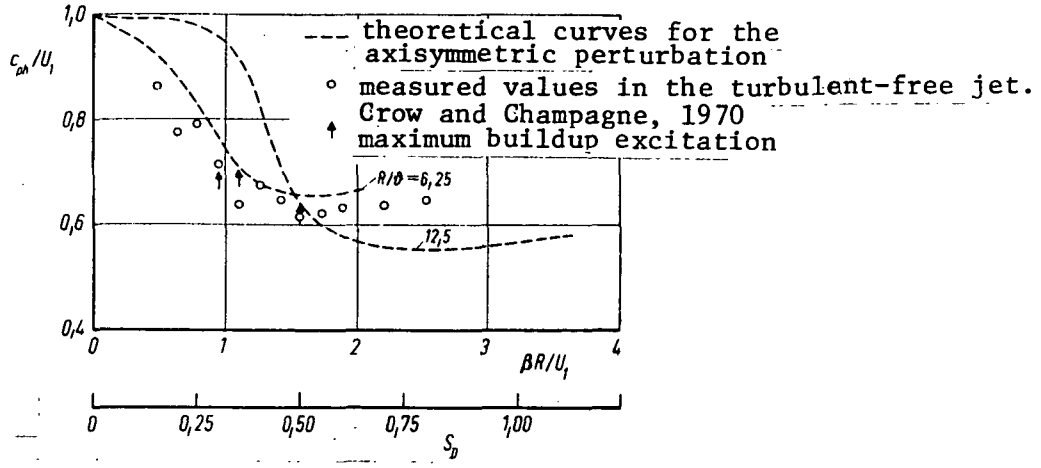

Figure 8: Measured phase velocity c_{ph} of the asymmetric perturbation in the turbulent free jet according to [44] as a function of the Strouhal number S_D compared with theoretical values for profile 2 and the free jet parameter values $R/\vartheta = 12{,}5$ and 6.25 (M = 0, T_o/T_1 = 1).

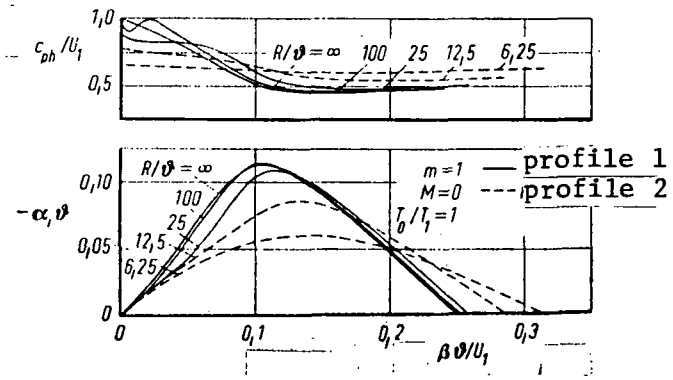

Figure 9: Phase velocity c_{ph} and buildup factor $-\alpha_i$ of the first azimuthal perturbation as a function of circular frequency β for various free jet parameter values R/ϑ (M = 0, $T_0/T_1 = 1$)

and m = 1 are quite different. The curves for the buildup factor for /326 large values of R/ϑ are approximately the same as for m = 0. For smaller values of R/ϑ, the maximum buildup for m = 1 drops somewhat more than for m = 0. However, the buildup for small $\beta\vartheta/U_1$ values is greater than for m = 0 because of the approximately linear increase of the curves, where the variation is approximatley parabolic. We therefore

can expect that for M → 0 and $R/\vartheta < 10$, the part of the first azimuth turbulence component in the round free jet is greater for very small Strouhal numbers for about $S_D < 0.2$ because of the greater instability, than for the axisymmetric component.

4.2 Influence of Mach Number on Instability of a Circular Free Jet

In the case of a plane shear layer, the instability becomes reduced for increasing Mach numbers, as H. Gropengeisser [26] and W. Blumen [39] have shown. The same is true for the circular free jet as Figure 10 shows for the axisymmetric perturbation. This shows the normalized buildup factor $-\alpha_i \vartheta$ as a function of $\beta\vartheta/U_1$ for the velocity profile 1 with $R/\vartheta = 100$ and for the velocity profile 2 for $R/\vartheta = 6{,}25$. The curve parameter is the Mach number M. The temperature ratio is T* = 1, the temperature distribution in the free jet, however, is not constant (see Figure 3). For both velocity profiles, as the Mach number increases, the unstable frequency range becomes smaller. The maximum buildup decreases and is displaced toward smaller values of $\beta\vartheta/U_1$.

The first azimuth perturbation with m = 1 has the same tendency as far as Mach number dependence is concerned. Their buildup factor

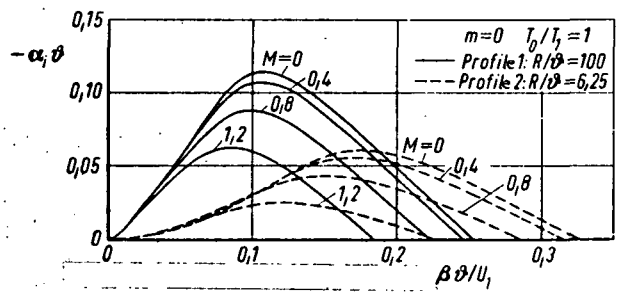

Figure 10: Buildup factor of the axisymmetric perturbation as a function of the circular frequency β for $R/\vartheta = 100$ and 6.25, and various Mach numbers M ($\gamma = 1{,}4$, $T_0/T_1 = 1$).

is shown in Figure 11 for the same velocity profiles and Mach numbers. Comparison of the curves for M = 1 and M = 0 in Figure 10 shows that for a free jet parameter $R/\vartheta = 100$, the curves are hardly different, as could be expected for $R/\vartheta \to \infty$. For $R/\vartheta = 6{,}25$, on the other hand, the buildup factor of the axisymmetric perturbation decreases more with increasing Mach number than for m = 1. For Mach numbers M > 0.8, the latter is excited more over the entire unstable frequency range than is the axisymmetric perturbation. This result is important for the instability of the turbulent free jet boundary layer, and leads to the

assumption that for high Mach numbers, in the entire Strouhal number range $S_D < 0.65$, the contribution of the first azimuth turbulence component increases, whereas the contribution of the axisymmetric component is reduced.

4.3 Influence of Temperature Ratio on the Instability of a Circular Free Jet

The influence of temperature on the instability of a plane shear layer which is the limiting case of a free jet for $R \to \infty$ was investigated by H. Gropengeisser [26]. He found that a hot jet which flows into cold surroundings is more unstable than isothermal jets. For the circular free jet with the boundary layer thickness $\vartheta = 0$, (cylindrical vortex layer), we find the same tendency for the perturbations built up in space [30]. However, we have a peculiar phenomenon in which for temperature ratios $T^* > 0.7$ the eigenvalue curves of the "regular" mode and of the first "irregular" mode exchange their variation over a certain frequency range. This means that it is no longer possible to uniquely define the "regular" and "irregular" modes, just like for $T^* > 0.7$. The same is true for finite values of the free jet parameter R/ϑ. Figure 12 shows the variation of the buildup factor of axisymmetric perturbations for the temperature ratio $T^* = 0.5$ and the velocity profile 1. The Mach number is $M = 0$. The curve $R/\vartheta = 20{,}000$ effectively coincides with the variation of the buildup factor for the plane shear layer. The value for the maximum buildup factor here is almost twice as great as for $T^* = 1$ in Figure 7. Therefore, a hot free jet is less stable than a cold one.

For $R/\vartheta = 50$ and 25 we see in Figure 12 clearly that the curve of the "regular" mode for values $\beta\vartheta/U_1$ below the maximum buildup become those of the "irregular" mode, which has a buildup $-\alpha_i > 0$ which is different from 0 for $\beta = 0$. The curves which start at $-\alpha_i = 0$ at $\beta = 0$, on the other hand, terminate at a certain value of $\beta\vartheta/U_1$, because there the corresponding wave number α_r becomes 0, which could be seen for /327 the "irregular" mode II for $T^* = 1$ in Figure 5.

However, these theoretical results for the hot free jet cannot be physically explained up to the present. Unfortunately, no experimental results about the instability of hot free jets are available, which would give information about the actual instability mechanism. Therefore we can assume that for a hot free jet, the instability for small

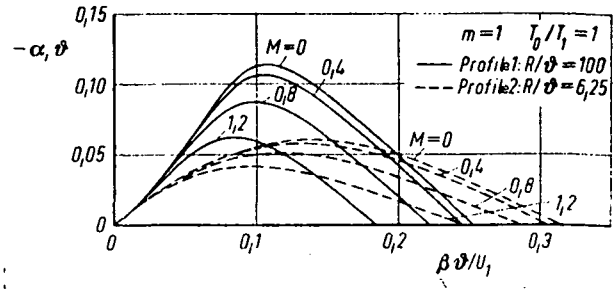

Figure 11: Buildup factor $-\alpha_i$ of the first aximuthal perturbation as a function of circular frequency β for $R/\vartheta = 100$ and 6.25 and various Mach numbers M ($\gamma = 1.4$, $T_o/T_i = 1$)

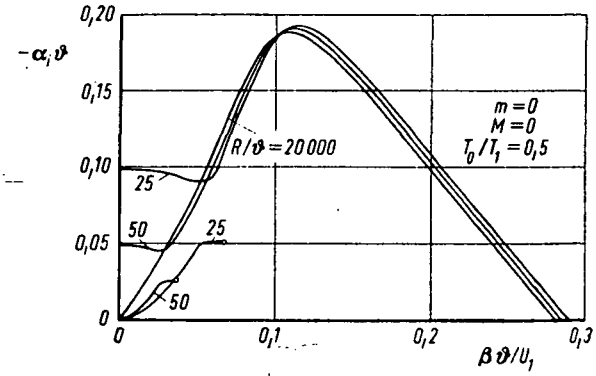

Figure 12: Buildup factor $-\alpha_i$ of the axisymmetric perturbation as a function of circular frequency β for hot free jets ($T_o/T_i = 0.5$) with various values of $R/\vartheta\,(M=0)$.

$\beta \vartheta/U_1$ values is much more complicated than for a cold jet, or that the assumption II of the theory about an infinite parallel flow is no longer applicable for a hot free jet.

†Institute for Turbulence Research (director: R. Wille) of the German Research and Test Facility for Aerodynamics and space flight D.F.V.L.R.)

5. REFERENCES

1. J. Tyndall: On the action of sonorous vibrations on gaseous and liquid jets. Phil. Mag. 33 (1867), p. 375-391.

2. Lord Rayleigh: On the instability of jets. Proc. London Math. Soc., 10 (1879), p. 4-13.

3. G. B. Brown: On vortex motion in gaseous jets and the origin of their sensitivity to sound. Proc. Phys. Soc. 47 (1935), p. 703-732.

4. R. Wille: Flow Phenomena in the transition region of ordered and unordered motion. Yearbook of Shipping History, 46 (1952), p. 176-187.

5. U. Domm: The hypothesis concerning the mechanism of turbulence creation. DVL-report, 23 (1956).

6. O. Wehrmann: Acoustic Control of the Turbulent Build-Up in a Free Jet. Yearbook 1957 of WGL, 102-108.

7. O. Wehrmann and R. Wille: Contributions to the Phenomenology of laminar-turbulent transition of a free jet for small Reynolds numbers. In: H. Gortler (Publisher): Grenzschichtforshung - Boundary Layer Research. Springer-Verlag, Berlin-Goettingen-Heidelberg, 1958, p. 387-404.

8. H. Fabian: Experimental investigations of the velocity fluctuation in the missing zone of a free jet near the nozzle mouth. DVL report, 122 (1960).

9. O. Wehrmann: Characteristics of separated cylindrical boundary layers. DVL-report 131 (1960).

10. H. Schade: Hydrodynamic stability theory of plane and axisymmetric parallel flows. DVL report 190 (1962).

11. H. Schade and A. Michalke: The creation of Vortices in a free boundary layer. Z. Flugwiss. 19 (1962), p. 147-154.

12. R. Wille: Contributions to the Phenomenology of Free Jets. Z. Flugwiss. II (1963, p. 222-233.

13. A. Michalke and H. Schade: Stability of Free Boundary Layer. Ing. -Arch. 33 (1963), p. 1-23.

14. A. Michalke: Intability and Nonlinear Development of a disturbed shear layer. Ing.-Arch. 33 (1964), pp. 264-276.

15. H. Schade: Contribution to the non-linear stability theory of inviscid shear layers. Physics of Fluids 7 (1964), p. 623-628.

16. A. Michalke: On the Inviscid instability of the hyperbolic-tangent velocity profile. J. Fluid Mechanics. 19 (1964), p. 543-556.

17. H. Schade: Introduction into Non-linear Hydrodynamic stability theory. Deutsche Luft- and Raumfahrt, FB 64-35, (1964).

18. A. Michalke and O. Wehrmann: Acoustic influence on free jet boundary layers. Proceedings of the International Council of the Aeronautical Sciences, Third Congress, Stockholm 1962. Spartan books, Inc., Washington, D.C., MacMillan & Co. Ltd., London, 1964, pp. 773-785.

19. A. Michalke: Vortex formation in a free boundary layer according to stability theory. J. Fluid Mech., 22 (1965), pp. 371-383.

20. A. Michalke: On spatially growing disturbances in an inviscid shear layer. J. Fluid Mech., 23 (1965), pp. 521-544.

21. P. Freymuth: The buildup of perturbations in separated laminar boundary layers. Deutsche Luft- and Raumfahrt, FB 66-02 (1966).

22. A. Michalke and R. Wille: Flow processes in the laminar turbulence transition range of free jet boundary layers. in : Applied Mechanics, Proceedings 11th International Congress Applied Mechanics, Munich, 1964. Springer-Verlag, Berlin/Heidelberg/ New York 1966, p. 962-972.

2. P. Freymuth: On the transition in a seperated laminated boundary layer. J. Fluid Mech. 25 (1966), S. 683-704.

24. A. Michalke and P. Freymuth: The instability and the formation of vortices in a free boundary layer. In: Separated flows. AGARD Conference Proc. 4 (1966), Part II, pp. 575-595.

25. A. Michalke and A. Timme: On the inviscid instability of certain two-dimensional vortex-type flows. J. Fluid Mech., 29, (1967), p. 647-666.

26. H. Gropengeisser: Contribution to the Stability of free boundary layers in compressible media. Deutsche luft- und Raumfahrt, FB 69-25, (1969).

27. A. Michalke: A note on spatially growing three-dimensional disturbances in a free shear layer. J. Fluid Mech., 38 (1969), p. 765-767.

28. A. Michalke: The influence of the vorticity distribution on the inviscid instability of a free shear layer. Fluid Dynamics Trans. 4 (1969), pp. 751-760 (published by Polish Academy of Sciences, Warsaw).

29. A. Michalke: The instability of free shear layers - A survey on the state of the art. Deutsche Luft- und Raumfahrt, Mitt. 70-04 (1970).

30. A. Michalke: A note on the spatial jet-instability of the compressible cylindrical vortex sheet. Deutsche Luft- und Raumfahrt, Mitt. 70-51 (1970).

31. A. J. Reynolds: Observations of a liquid-to-liquid jet. J. Fluid Mech., 14 (1962), p. 552-556.

32. H. A. Becker and T. A. Massaro: Vortex evaluation in a round jet. J. Fluid Mech. 31 (1968), p. 435-448.

33. G. S. Beavers and T. A. Wilson: Vortex growth in jets. J. Fluid Mech. 44 (1970), p. 97-112.

34. A. B. C. Anderson: Structure and velocity of the periodic vortex-ring flow pattern of a primary Pfeifenton (pipe tone) jet. J. Acoust. Soc. America 27 (1955), p. 1048-1053.

35. A. B. C. Anderson: Vortex-ring structure-transition in a jet emitting discrete acoustic frequencies. J. Acoust. Soc. America 28 (1956), p. 914-921.

36. H. Sato: The stability and transition of a two-dimensional jet. J. Fluid Mech. 7 (1960), p. 53-80.

37. M. Gaster: A note on the relation between temporally-increasing and spatially-increasing disturbances in hydrodynamic stability. J. Fluid Mech., 14 (1962), p. 222-224.

38. M. Gaster: The role of spatially growing waves in the theory of hydrodynamic stability. In: D. Kuchemann and L. H. G. Sterne (Publisher). Progress in Aeronautical Sciences, Vol. 6, Pergamon Press, Oxford/London/Edinburgh/New York/Paris/Frankfurt, 1965, pp. 251-270.

39. W. Blumen: Shear layer instability of an inviscid compressible fluid. J. Fluid Mech., 40 (1970), pp. 769-781.

40. G. K. Batchelor and A. E. Gill: Analysis of the stability of axisymmetric jets. J. Fluid Mech., 14 (1962), p. 529-551.

41. M. Lessen, J. A. Fox, H. M. Zein: The instability of inviscid jets and wakes in compressible fluid. J. Fluid Mech., 21 (1965), p. 129-143.

42. A. E. Gill: Instabilities of "top hat" jets and wakes in compressible fluids. Physics of Fluids 8 (1965), p. 1428-1430.

43. T. Kambe: The stability of an axisymmetric jet with parabolic profile. J. Phys. Soc. Japan 26 (1969), p. 566-575.

44. S. C. Crow and F. H. Champagne: Orderly Structure in Jet Turbulence. Boeing Sci. Res. Lab, Document D 1-82-0991 (1970).

45. P. G. Drazin and L. N. Howard: The instability to long waves of unbounded inviscid flow. J. Flouid Mech. 14 (1962), pp. 257-283.